Chapter 3

A Novel Genetic Circuit Supports Laboratory Automation and High Throughput Monitoring of Inflammation in Living Human Cells

Natalie Duong, Kevin Curley, Mai Anh Do, Daniel Levy and Biao Lu

Additional information is available at the end of the chapter

http://dx.doi.org/10.5772/intechopen.78568

Abstract

Genetically encoded reporter circuits have been revolutionizing our ability to monitor, manipulate, and visualize specific cellular responses to a variety of environmental stimuli. However, the development of genetic circuits that enable both high throughput (HTP) application and laboratory automation remains challenging. In this report, we describe a novel dual-reporter circuit that utilizes a secretory Gaussia luciferase (Gluc) and a green fluorescent protein (GFP) for monitoring inflammatory signaling, a fundamental process in many life events. We designed and built this genetic circuit into a simple adeno-associated viral (AAV) vector, which is suitable for both simple transfection and efficient transduction protocols. We demonstrated high sensitivity and specificity of this new circuit and its ability to monitor a broad range of inflammatory response in various human cell models. Importantly, this novel system is simple, robust, and readily adaptable to HTP applications and laboratory automation including fluorescence activated cell sorting (FACS) and microplate reader analysis. By combining both GFP and Gluc in one genetic circuit, our new dual-reporter circuit provides an easy and powerful tool for monitoring and quantifying inflammatory signals in various mammalian cells.

Keywords: inflammation, NF-κB, Gaussia luciferase, TNFα, AAV, GFP

1. Introduction

Genetically encoded reporters such as fluorescent and bioluminescent proteins have achieved widespread success as useful research tools in life sciences, including cell biology [1–3], oncology

[4, 5], cardiology [6, 7], neurology [8, 9], as well as infection and inflammation studies [10, 11]. Because of their sensitivity in quantitative measurement, both fluorescent and bioluminescent proteins remain the top choices for monitoring live cell processes in mammals. The most commonly used reporters include green/red fluorescent proteins or their genetic derivatives (GFP, RFP, YFP or mCherry) [12–14]. Insect or marine bioluminescent proteins (Firefly luciferase or Renilla/Gaussia luciferase) are used as well [15–17]. Through codon optimization, these reporters have been genetically engineered to monitor many physiological and disease processes such as cell communications [18, 19], protein and exosome secretion [20, 21], viral infection, inflammation, and apoptosis [5, 11, 22]. In most situations, a single type of reporter may provide better sensitivity and specificity over traditional methods such as Western blot analysis or polymerase chain reactions (PCRs). For example, fluorescent proteins may provide handy real-time monitoring when a fluorescence microscope is available. However, the signal quantification is less convenient and often requires sophisticated software or expensive FACS equipment [9, 23, 24]. On the other hand, the bioluminescent reporter is easily quantifiable and can be made amenable to laboratory automation by using a less expensive luminometer [18, 25, 26]. Therefore, the combination of both types of reporters may be superior, allowing for both visual monitoring and laboratory automation.

Recently, we have developed a novel dual-reporter circuit from the marine GFP and the firefly luciferase (Fluc) and demonstrated their usage in studying gene regulation and cell signaling in mammalian cells [27]. Additionally, we and others have shown that the marine *Gaussia princeps* termed Gaussia luciferase (Gluc) has many advantages over Fluc, including secretory nature, higher assay sensitivity and specificity [17, 25, 28]. Notably, secreted Gluc activity can be easily assayed by withdrawing a portion of conditioned medium, allowing real-time monitoring while avoiding the cell lysis procedures often required for the quantification of Fluc reporter.

In this chapter, we describe the design and validation of a novel AAV vector-based dual-reporter format by a combination of GFP and Gluc for high throughput monitoring of inflammation in human cells. This new circuit has high sensitivity and specificity with little background noise in reporting inflammatory response. We demonstrate that the GFP allows for real-time monitoring and produces high-content data sets at individual cell levels using fluorescence microscope or FACS. In parallel, the secretory Gluc allows for the monitoring of inflammatory response at population levels and enables HTP analysis and laboratory automation with a luminometer or microplate reader. Together, this dual-reporter provides a robust and high throughput means to study inflammation in human cell or animal models.

2. Materials and methods

2.1. Materials

Inflammatory cytokine TNFα was obtained from R&D Systems (Minneapolis, MN). Phorbol-12-myristate 13-acetate (PMA) was obtained from MilliporeSigma (St. Lois, MO). Luciferase

assay reagent and fetal bovine serum (FBS) were obtained from ThermoFisher (Waltham, MA). AAV-DJ capsid protein and the helper free viral packaging system were obtained from Cell Biolabs (San Diego, CA). The serum-free UltraCULTRE complete medium was obtained from Lonza (Anaheim, CA).

2.2. Genetic circuit construction

The AAV-based dual-reporter circuit was constructed by DNA synthesis and a fusion technology as previously reported [24, 29]. The reporter circuit was flanked by inverted terminal repeats (ITRs). These two ITRs were synthesized by direct DNA synthesis from Genscript (Piscataway, NJ). We then built the genetic cassette according to the configuration from the 5′ to 3′-end: the transcription factor response elements (TREs) of NF-κB, a minimal CMV promoter sequences (mCMV), a dual-reporter with a self-splicing peptide (Gluc-T2A-GFP), the poly adenylation signaling sequences (Poly-A) (NF-κB reporter, GenBank Accession Number: MG786368). To evaluate the background noise, basal transcription activity and the inducible signal range, a promoterless reporter (background noise, MG786370), a minimal promoter (basal transcription activity, GenBank Accession Number: MG786371), and a full promoter CMV (signal range, GenBank Accession Number: MG786372) were built in a similar format. To assess the specificity, a dual-reporter responsive to growth factors (AP-1 reporter, GenBank Accession Number: MG786369) but not inflammatory stimuli was similarly designed and constructed. Final constructs were sequence-verified from ITR to ITR, and the annotated sequences can be retrieved from GenBank (MG786368–72).

2.3. Cell culture and transfection

Human embryonic kidney cells (HEK293), human liver cancer line (HepG2) and human glioblastoma line (U87) were obtained from ATCC (Manassas, VA). Cells were cultured in DMEM supplemented with 10% FBS, 2 mM GlutaMax and penicillin-streptomycin 100 U/mL. All cells were culture at 370C with 95% humid air and 5% CO_2.

Cell culture transfections were conducted in 6-well plates as reported [27]. Cells growing at 50–70% confluency were transfected by combining reporter DNA (1–2.5 μg/well) with Lipofectamine (Thermo-Fisher) or FuGene 6 transfection reagents (Promega) for 24–72 h. Cells were then switched to fresh medium for cytokine treatment.

2.4. Recombinant AAV production and titration

Reporter AAV were produced by transfecting HEK293 cells as reported [27]. Cells on culture dishes were transfected with a mixture of reporter DNA and helper AAV-reporter plasmids expressing Rep and Cap proteins. Twenty-four hours after the transfection, culture medium was changed to allow production of viral particles for additional forty-eight hours. The recombinant AAV viruses were prepared from the conditioned medium using an AAV concentration reagent according to the manufacturer's instruction (System Biosciences, Palo Alto, CA). All AAV reporter viruses were packaged with AAV-DJ capsids, which have broad tropism in transduction [30].

Viral titration and multiplicity of infection (MOI) were determined by performing green cell fluorescent assay and PCR as reported [27, 31, 32]. Briefly, HEK293 cells on 12-well plates were transduced with serial dilutions of fCMV-Gluc-T2A-GFP control viruses. After 72 h, GFP-positive cells were visually scored under a fluorescence microscope. MOI of control virus was determined by GFP positivity of the transduced cells, while the MOI of reporter viruses was estimated by comparing the relative copy numbers of the reporter viruses to those of the GFP-positive control viruses [27].

2.5. Gaussia luciferase assay

Gaussia luciferase activity was assayed by a luminometer (Promega, Fitchburg, WI) as previously reported [18, 24]. Briefly, conditioned medium from treated cells were collected and subsequently cleared by centrifugation at 12,000 rpm for 5 min. The cleared supernatants were used for Gluc assay. For Gluc activities quantification, 100 μL of substrate was added to 5 or 10 μL of the conditioned medium and relative light units were recorded instantaneously [25].

2.6. Live fluorescence microscopy

Images of living cells were typically taken using fluorescence microscopy as reported [33]. To show the intensity of GFP expression, both fluorescent and phase contrast images were recorded. To compare expression levels of GFP, identical parameters including the exposure time, contrast and gain were kept identical within each set of experiments. When the fluorescence intensity was low, images were equally adjusted to show the relative GFP intensity.

2.7. Fluorescence activated cell sorting analysis (FACS)

Cultured HEK293 cells were sorted and quantified by using the Accuri C6 Cytometry (BD Biosciences, San Jose, CA). More than 10,000 events were recorded via a GFP channel. Triplicate samples were analyzed to ensure consistency in results. Data were processed by CFlow Plus software.

2.8. GFP quantification by microplate reader

Relative GFP intensity was quantified using a Microplate Reader (BMG Labtech) following the cytokine treatment. To reduce background noise level, the conditioned media were removed and cells were washed with phosphate buffer. The relative GFP intensity was recorded for both treatment and control groups. For each sample, nine areas were measured and averaged by the OMEG 3.00R2 software.

2.9. Data collection and presentation

Human cells were monitored in real-time under fluorescence microscopy. Fluorescent and phase contrast images were recorded under the same experimental conditions. For Gaussia luciferase assay, GFP quantification, and FACS analysis, the data are reported as mean ± SD (n = 3), unless stated otherwise.

http://dx.doi.org/10.5772/intechopen.78568

3. Results

3.1. Design and construction of AAV-based dual reporter circuits for monitoring inflammation in living human cells

Temporal monitoring and quantifying of inflammatory response at individual cell levels or within tissues is highly desirable [34, 35]. To accomplish this goal, we developed a new format of genetic circuit composed of transcription response elements (TREs), a minimal promoter (mCMV) and a dual-reporter (Gluc and GFP) (**Figure 1A**). According to this design, the TREs will respond to the binding of activated transcription factors such as NFκB; thus, they can switch the expression of reporter genes from an off-status to an on-status (**Figure 1A**). Since different signaling molecules may elicit distinct transcription factors (TFs). A careful choice of TREs will enable the construction of different genetic circuits for signaling monitoring. For instance, by using the binding sequences of NFκB as TREs (**Figure 1B**), this unique circuit may be able to monitor inflammation processes. Preferably, this genetic circuit will respond specifically to inflammatory molecules such as TNFα [36–38]. Taking advantage of different features of reporter proteins, the cell response can be real-time monitored by a number of HTP methods. For example, GFP may be imaged by fluorescence microscopy or quantified by microplate reader or

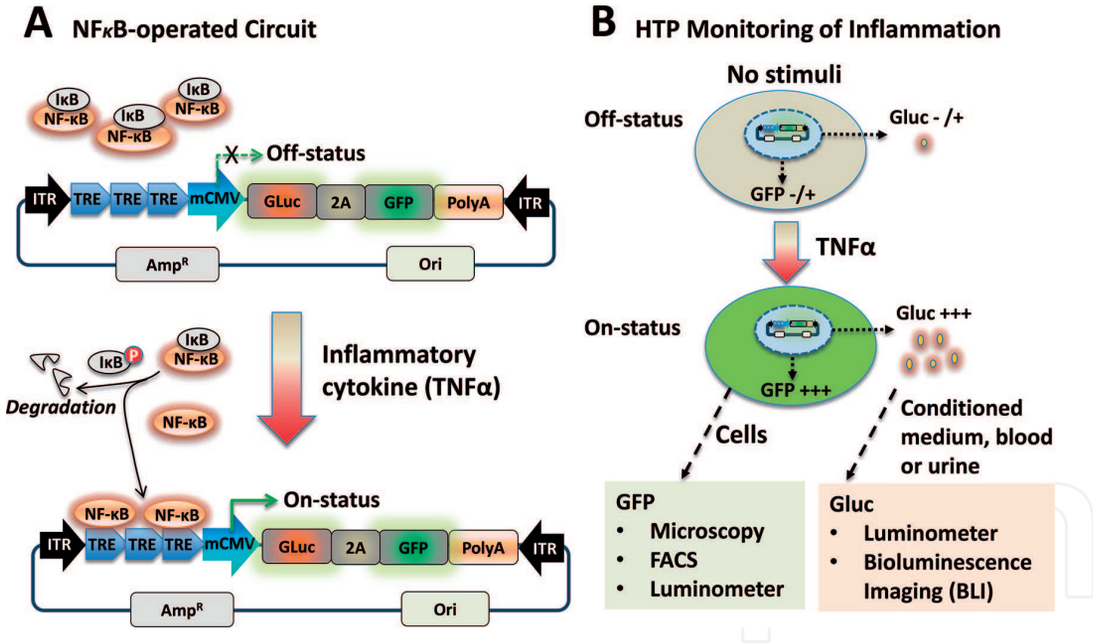

Figure 1. System design and workflow of AAV-based dual reporters for high throughput monitoring of inflammatory response in human cells. (A) Schematic illustration of genetic circuit of the AAV-based dual reporter. The genetic circuit (5′ → 3′) is composed of the transcriptional responding elements (TREs), the minimal CMV promoter (mCMV), a chimeric gene coding dual reporter proteins Gluc and GFP with a T2A (self-cleavage peptide). Depending on the availability of transcription factor (NF-κB), this inflammatory circuit may be either in an off-status with only minimal expression of reporters when no NF-κB binds to its TREs (upper panel), or in an on-status with a high level of expression when NF-κB binds to its TREs stimulated by inflammatory cytokine TNFα (lower panel). (B) Workflow for HTP monitoring of inflammatory response with GFP and Gluc. Cellular response to inflammatory stimuli can be monitored and quantified by GFP reporter (high content microscopy, FACS, microplate reader, or luminometer). Alternatively, inflammatory signaling can also be quantified by Gluc reporter from a portion of conditioned medium (Luminometer or bioluminescent imaging, BLI).

FACS. Alternatively, secreted Gluc activity can be easily quantified by assaying a portion of conditioned medium, blood, or urine. Because the wave length of Gluc emission is longer than 600 nm, Gluc becomes a preferred imager for in vivo bioluminescence imaging (BLI) (**Figure 1B**).

To test our new system, we built two reporter circuits to monitor either inflammatory processes (NFκB) or cell growth signaling (AP1). Typically, 4–6 tandem reporters of TREs can be joined together via 6-bp linkers [27]. These TREs were inserted the upstream of the mCMV-driven dual-reporter. This reporter circuit was flanked with ITR to allow AAV packaging and production.

3.2. Functional validation of the dual-reporter circuit

To determine the background noise, basal transcription activity, inducible signal range, and the signal-to-noise ratio of the new circuit, we further designed and constructed three additional vectors: (1) a promoterless vector to assess the background noise; (2) a minimal promoter vector to assess the basal activity; and (3) a full-length CMV promoter to assess the signal range (**Figure 2A**). We transfected these reporters into HEK293 and monitored the appearance of GFP and red fluorescent protein (RFP), which was co-transfected and served as an invariable control (driven by a constitutive EF1α promoter) (**Figure 2B**). As predicted, cells transfected by the promoterless circuit remained GFP negative for 48 h, indicating little background noise of this new AAV reporter circuit (**Figure 2B**, **a**, **g**). For the minimal promoter circuit, few cells were weakly positive for GFP, indicating low levels of basal expression (**Figure 2B**, **b**, **h**). In contrast, ∼80% of cells exhibited strong GFP fluorescence in the fCMV group (24–48 h) (**Figure 2B**, **c**, **i**). However, under the same experimental condition, the steady expression levels of control RFP remained consistent among different groups for both 24 h (**Figure 2B**, **d–f**) and 48 h (**Figure 2B**, **j–l**), suggesting the differential expression of GFP was attributed to the promoter usage rather than the differences caused by transfection discrepancy. Together, these data validated the functionality of our new circuit and confirmed that GFP could be used for reporting signaling strength in living human cells.

In parallel, we also examined the Gluc activities from the conditioned media to determine if the Gluc activities were similarly regulated depending on the promoter types. As shown in **Figure 2C**, the promoterless circuit showed a very low background noise while the mCMV promoter circuit exhibited a significant increase in Gluc activities (∼30.9-fold at 24 h, ∼56.9-fold at 48 h). A marked ∼2255- or ∼3847-fold increase in Gluc activity was recorded for the fCMV promoter circuit. These data confirmed that the new reporter format has low levels of background noise and a broad signal range with a signal-to-noise ratio of ∼3847:1.

3.3. Specificity of the dual-reporter circuit in monitoring inflammation using transfection protocol

Next, we tested whether the dual-reporter system was specific in monitoring inflammation with a commonly used transfection protocol. We conducted a comparative study on two distinctive pathways, the inflammation (NFκB) and cell growth (AP-1). These two pathways have been

http://dx.doi.org/10.5772/intechopen.78568

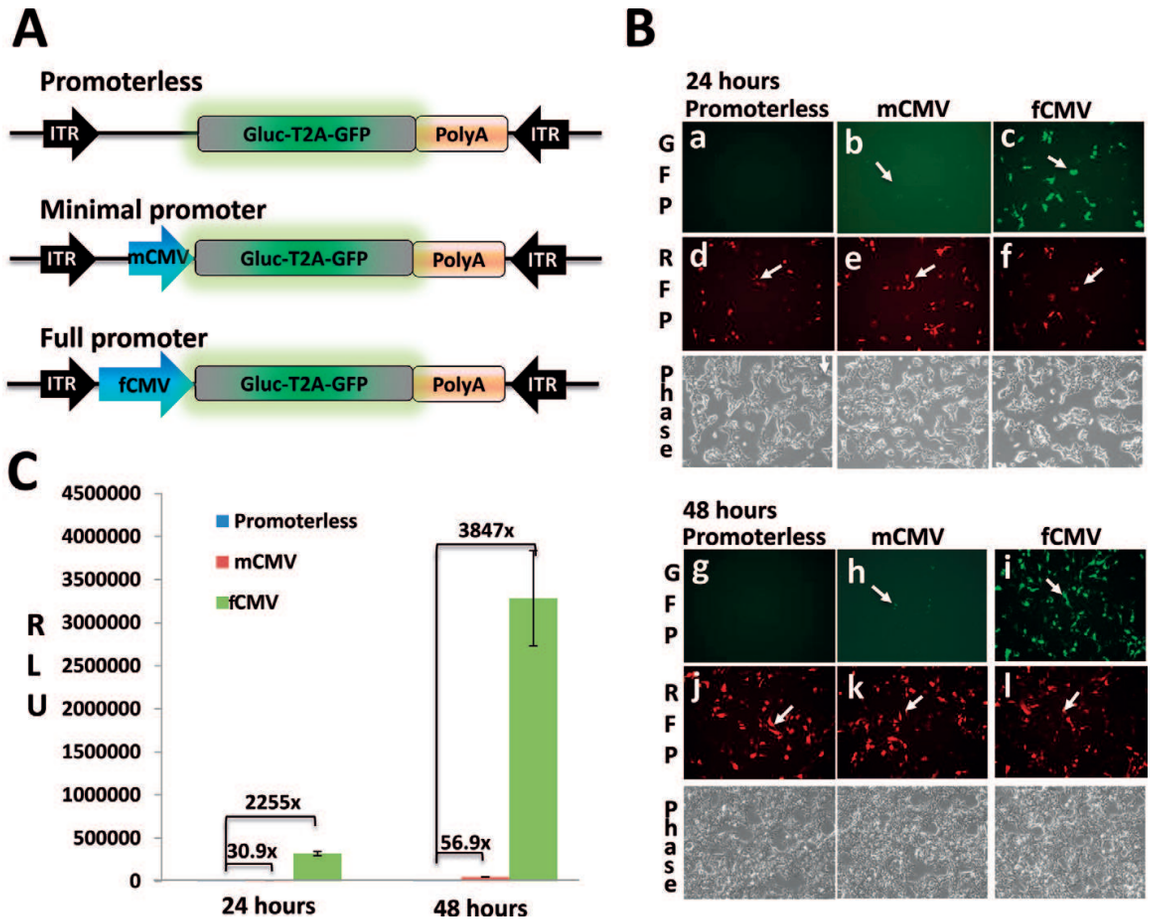

Figure 2. System setup and performance analysis. (A) Design and construction of three AAV-based dual reporters for system testing. The dual-reporter circuit is flanked by inverted terminal repeats (ITR), which allows for packaging into recombinant AAV. Promoterless, minimal promoter (mCMV) and full CMV (CMV)-driven dual reporter circuit are shown from top to bottom. (B) Expression of dual-reporters in live HEK293 cells. The GFP expression (green) in HEK293 cells were recorded with a fluorescence microscope following transfections of either a promoterless, an mCMV, or an fCMV-driven reporter at 24 h (a–c) and 48 h (g–i), which were co-transfected with a positive control plasmid DNA expressing RFP (d–f for 24 h; j–l for 48 h). Arrows indicate GFP- or RFP-positive cells. The bottom panels show the corresponding phase-contrast images for each group. (C) The Gluc activity from the conditioned medium was determined by a luciferase assay following the transfection of three reporters at the same time points. The luciferase activity was expressed as relative light units (RLU), normalized against protein input, and presented as fold increase over untreated control (mean ± SD, n = 3) with statistical significance of $P<0.001$, using student's T-test. The bottoms panels are representative phase-contrast images for each treatment group.

shown to be specifically activated by proinflammatory cytokine (TNFα) and cancer promoting reagent (PMA), respectively [18, 39]. Accordingly, we co-transfected HEK293 cells using each of these reporters along with EF1α-driven RFP as invariable reference to determine specific effects of TNFα and PMA on reporter activations. After cells were transfected with NFκB-Gluc-2A-GFP reporter, treatment of cells with 10 ng/mL TNFα induced a marked increase in GFP levels (**Figure 3A**, **b**). In parallel, a 42-fold increase in Gluc activity was detected, indicating an activation of the inflammatory pathway (**Figure 3B**). As expected, very few GFP-positive cells were present in the wells treated with PMA, suggesting specific activation of NFκB by TNFα but not PMA (**Figure 3A**, **c**). Again, no significant change in Gluc activities was observed in mock

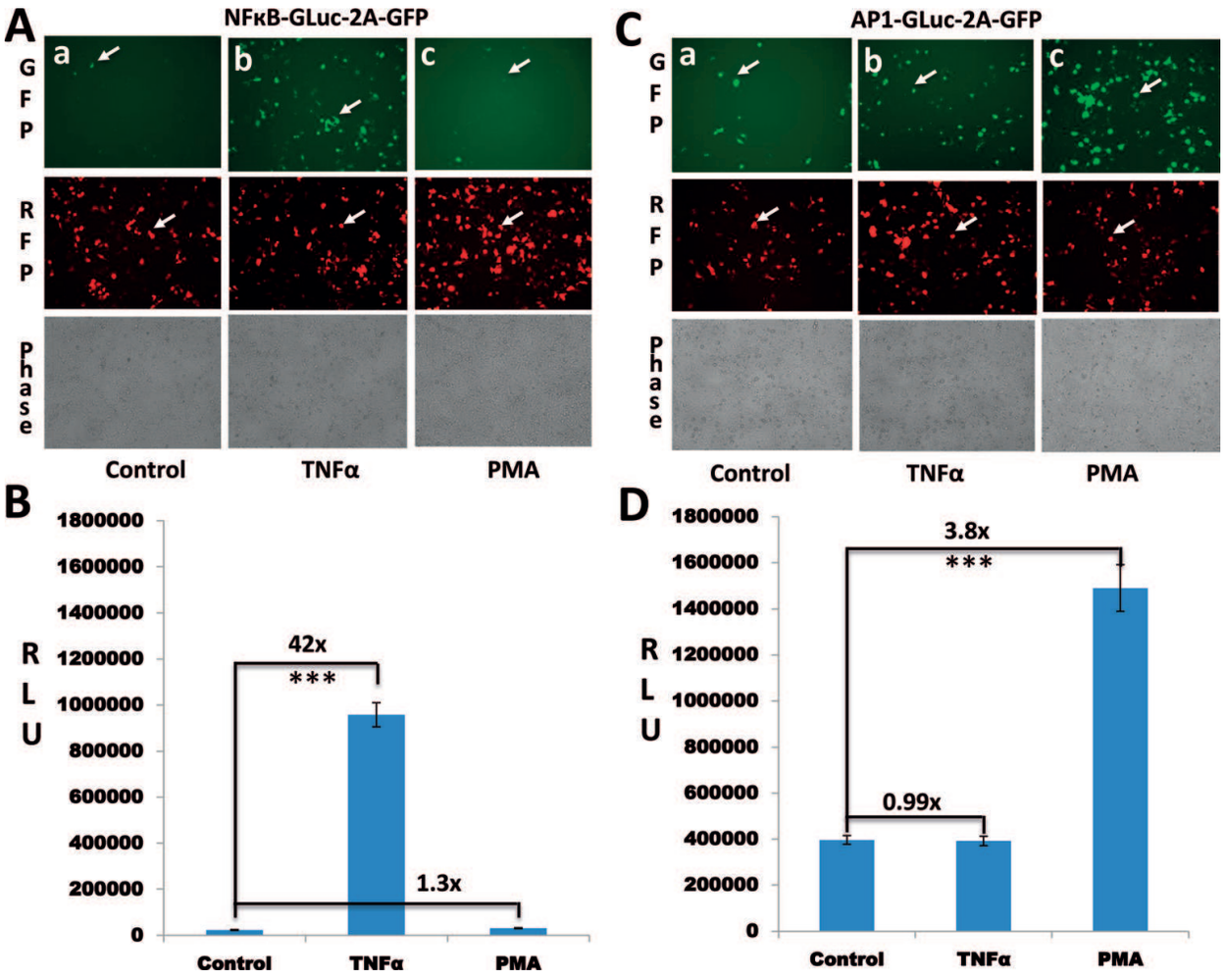

Figure 3. The specificity of the AAV-based dual-reporters by transfection. HEK293 cells were transfected with NF-κB reporter for 24 h. Cells were then switched to low serum medium in the presence or absence of either TNFα (10 ng/mL) or PMA (50 ng/mL) for 24 h. The images of GFP (A: a–c), RFP (A: d–e), and phase (A: lower panel) were recorded 24 h after the treatment. The corresponding luciferase activity was assayed using the conditioned medium collected from a control, TNFα or PMA treatment group (B). In a separate set of experiments, HEK293 cells were transfected with AP-1 reporters for 24 h, followed by the treatment of either TNFα (10 ng/mL) or PMA (50 ng/mL) for additional 24 h. The GFP (B: a-c), RFP (B: d-e), and phase (B: lower panel) images were recorded and the corresponding luciferase activity was also assayed and graphed (D). Arrows indicates the GFP- or RFP-positive cells. The luciferase activity was expressed as relative light units (RLU) and presented as fold increase over untreated control (mean ± SD, n = 3). *** denotes P<0.001, using student's T-test.

control or cells treated with PMA (**Figure 3B**). Conversely, after cells were transfected with the AP1-Gluc-2A-GFP reporter, treatment of cells with 50 ng/mL PMA induced a significant increase in GFP levels (**Figure 3C**, **c**), in line with a 3.8-fold increase in Gluc activities (**Figure 3D**). In contrast, neither mock-control (**Figure 3C**, **a**) nor TNFα (**Figure 3C**, **b**) caused any significant changes in the expression levels of GFP or Gluc (**Figure 3D**). Additionally, the co-transfected invariable reference RFP showed little changes among different groups (**Figure 3A**, **C**, middle panels), excluding the possibility that such differences were caused by discrepancies in transfection efficiency. Taken together, these results confirm the specificity of our new reporter circuit in monitoring inflammation using a simple transfection protocol.

http://dx.doi.org/10.5772/intechopen.78568

3.4. Monitoring cell signaling response using an AAV transduction protocol

Following successful monitoring of cell signaling with a transfection protocol, we further test whether the new AAV-based circuit could be successfully packaged into delivery viral particles to deliver the reporter circuit to various cells [40–42]. For virus packaging, we used our established protocol to generate recombinant reporter viruses [27]. For cell transduction, packaged viruses (~ 1× MOI viruses) were used to transduce HEK293 cells for 24 h. Following the transduction, cells were washed and switched to UltraCULTURE for the treatment of TNFα or PMA. Similar to the transfection experiment, the NFκB reporter circuit showed a marked increase in Gluc activity (85-fold over control) in response to the TNFα treatment but not PMA (**Figure 4A**). Conversely, the AP-1 reporter circuit showed a smaller but significant increase in Gluc activity (9.6-fold over control) for the treatment of PMA but not TNFα (**Figure 4B**). These results validated the specificity of this dual-reporter using a highly effective

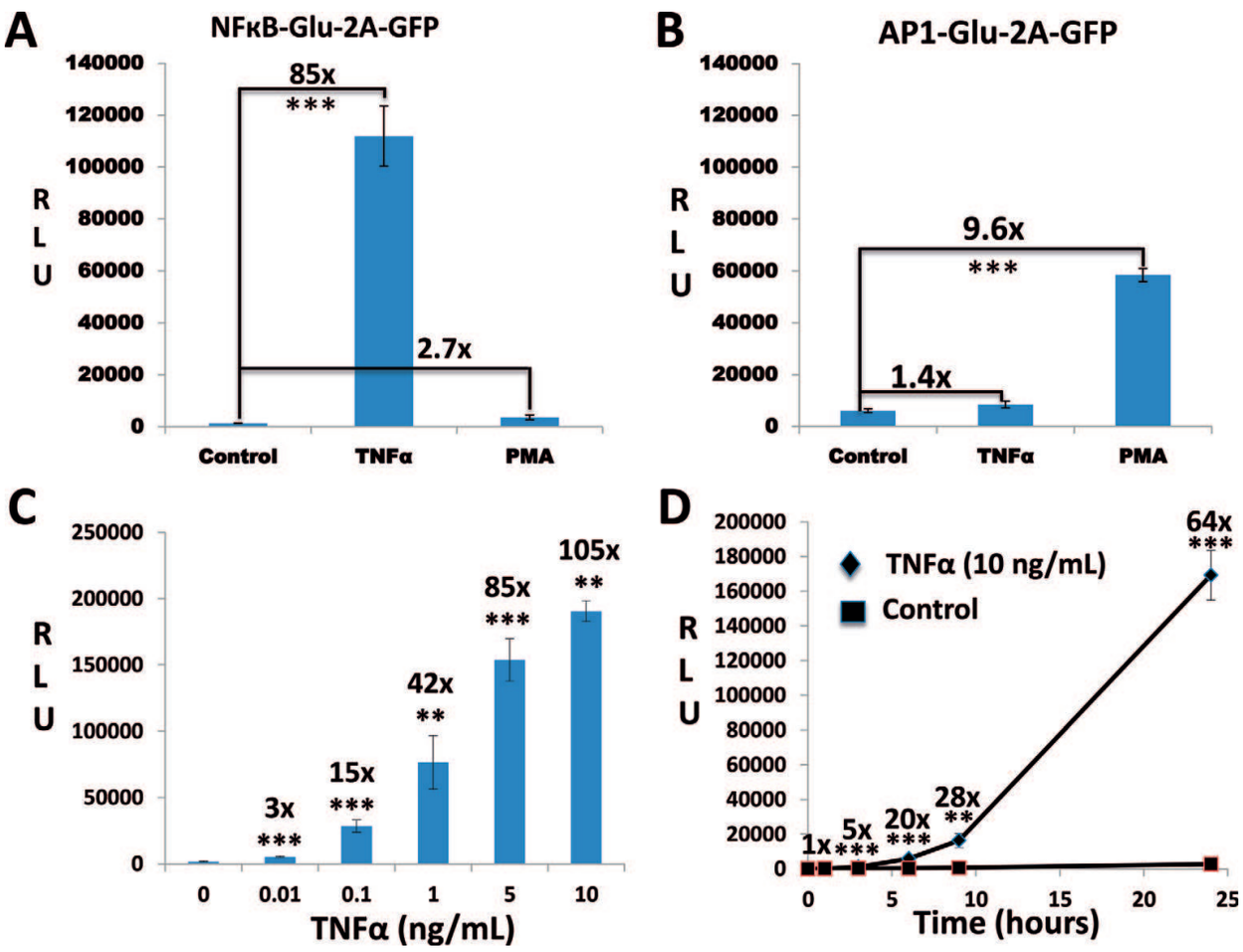

Figure 4. The specificity of AAV-based reporters by transduction. HEK293 cells were transduced with either NFκB (A) or AP-1 (B) reporter AAV (MOI = 1) for 24 h. Cells were then switched to low serum medium in the presence or absence of TNFα (10 ng/mL) or PMA (50 ng/mL) for additional 24 h. In separate experiments, following 24 h transduction with NFκB reporter AAV, HEK293 cells were subject to either the treatment of increasing concentration of TNFα (0, 0.1, 1, 5 10, and 50 ng/mL) for 24 h (C), or in the presence of TNFα (10 ng/mL) for 0, 3, 7, 24, 48, and 72 h (D).The luciferase activity was determined using conditioned medium, and expressed as relative light units (RLU) or presented as fold increase over untreated control (mean ± SD, n = 3). ** denotes P<0.01, while *** denotes P<0.001, using student's T-test.

transduction protocol. Consistent with low basal level of Gluc activities, we also observed a low GFP expression in control cells, which increased in their intensities in response to TNFα treatment but not to PMA. Likewise, the GFP intensity increased in response to PMA but not to TNFα treatment in the AP-1 system, indicating specific response to its corresponding singling stimuli. It is worth noting that both GFP intensity and Gluc activity appeared to be low for cells with transduction in comparison to transfection. However, the relative fold-increase of Gluc appeared to be more prominent (85-fold vs. 42-fold increase for NF-κB and 9.6-fold vs. 3.8-fold increase for AP-1), which suggests that the lower background noise may increase the detection sensitivity using viral transduction protocol. Nevertheless, our data support the notion the new format of reporter circuit could be used to monitor and quantify inflammation or cell growth signaling by either simple transfection or highly efficient transduction protocols.

3.5. Sensitive and real-time monitoring of inflammatory response

We next performed the dose-response and time-course experiments to examine the sensitivity of our inflammatory reporter circuits in HEK293 cells. Following the transduction of cells with either AAV-based NFκB reporter or control plasmid for 24 h, cells were treated with incremental amount of TNFα (0.01, 0.1, 1, 5, and 10 ng/mL) for 24 h. As low as 0.01 ng/mL TNFα induces a significant rise of Gluc activity (3-fold over control, **Figure 4C**). As expected, higher TNFα concentrations (0.1–10 ng/mL) elicited more robust responses (15–105-fold over control) in a dose-dependent fashion (**Figure 4C**). In agreement with Gluc activities, GFP images exhibited a similar pattern of dose-dependent increase of GFP expression levels in responding to TNFα.

To temporally examine the activation of the NFκB reporter, we conducted a time-course study on the effects of TNFα using the established transduction protocol. We used a dosage of 10 ng/mL of TNFα because this dosage can induce a robust response in the above dose-response experiments. As early as 3 h following TNFα treatment, Gluc activity started to rise significantly (5-fold over control, **Figure 4D**). During the first 24 h, Gluc activity steadily increased (5–64-fold over control) (**Figure 4D**). Together, these results show that our new dual-reporter responds to inflammatory stimuli in both a dose- and time-dependent fashion, hence demonstrated the usefulness of the secreted Gluc for temporal monitoring of inflammation with our new reporter circuit in living human cells.

3.6. Coupling of dual-reporter with cytometer and automation-compatible microplate reader

To further explore whether our new dual-reporter circuit is amenable to HTP applications, we conducted a series of high content experiments that consisted of multiple dose- and time-course studies. Following the transduction of AAV-based NFκB reporters, cells were treated with incremental concentrations of TNFα (0, 0.01, 0.1, 1, 5, 25, 100 ng/mL). At multiple time-points (0, 1, 3, 6, 9, 24, 32, and 48 h), a small portion of culture medium was collected to determine the Gluc activity. As shown in **Figure 5A**, both time- and dose-dependent responses to the treatment of TNFα were detected. However, the cellular response to TNFα appeared to be attenuated in the following 24–48 h, indicating the maximum possible stimulation achieved at 24 h time-point. It is important to note that cellular response demonstrated a typical early response (**Figure 5B**). At doses of 0.1 ng/mL and above, significant increases (**Figure 5B**) in Gluc activities

http://dx.doi.org/10.5772/intechopen.78568

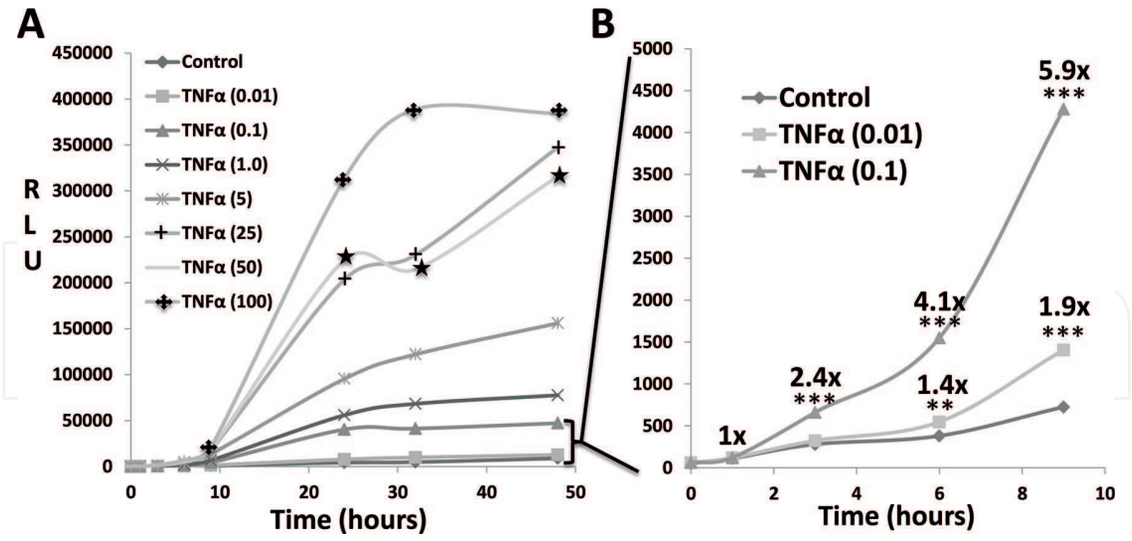

Figure 5. (A) HEK293 cells respond to TNFα stimuli in a time- and dose-dependent manner. Following transduction with NF-κB reporter virus (MOI = 1) for 24 h, HEK293 cells were treated with increasing concentration of TNFα (0, 0.01, 0.1, 1, 5, 10, 25, 50 and 100 ng/mL). A small portion of conditioned medium was collected at the indicated time-points (0, 1, 3, 6 and 9 h). The luciferase activity was determined using the conditioned medium, and expressed as relative light units (RLU) or presented as fold increase over untreated control (mean ± SD, n = 3). (B) Inset of control and treatment concentrations of 0.1 and 0.01 ng/ml. ** denotes P<0.01, while *** denotes P<0.001, using student's T-test.

were apparent. Even at the lowest dose of 0.01 ng/mL, a small increase (1.4-fold over control) in Gluc activities was detected at 6 h (**Figure 5B**), supporting a receptor-mediated quick activation model. Additionally, the secreted reporter Gluc enabled us to conduct these multi-dose (eight dosages) and multi-times (8 time-points) experiments in a triplicate format (three biological repeats), yielding a total of 192 data points, rendering a reliable and informative pattern of response.

We next examined the individual cell response to inflammatory cytokines using FACS as a HTP tool. HEK293 cells were transduced with AAV-based NFκB reporters, and the GFP emission was quantified by FACS. As expected, cells in the background group (mock transfection) were GFP-negative (**Figure 6A**, left panel), while reporter-transduced cells showed weak GFP expression in the absence of TNFα (**Figure 6A**, middle panel), but high GFP expression in the TNFα-treatment group (**Figure 6A**, right panel), demonstrating a robust cellular response. In parallel, our cytometry data revealed high intensity of GFP signal at individual cell levels: 0% in background group vs. 26% in control group vs. 83.6% in TNFα group (**Figure 6B**). A marked shift of GFP intensity following TNFα treatment was apparent when these graphs were merged (**Figure 6C**). Additionally, the individual response could also be summarized and averaged to evaluate cellular response as a heterogeneous population, which showed ~40-fold increase in TNFα group over control (**Figure 6D**). Together, our results demonstrated that flow cytometry can be used to assess inflammatory response at both individual cell and population levels using our novel reporter circuit.

Next, we examined whether a more commonly available microplate reader can be an alternative readout tool compared to the expensive cytometer for GFP quantification. Following the transfection of HEK293 cells with our NFκB reporter, the GFP intensity was recorded by fluorescent microscopy and the GFP emission was quantified with a microplate reader equipped

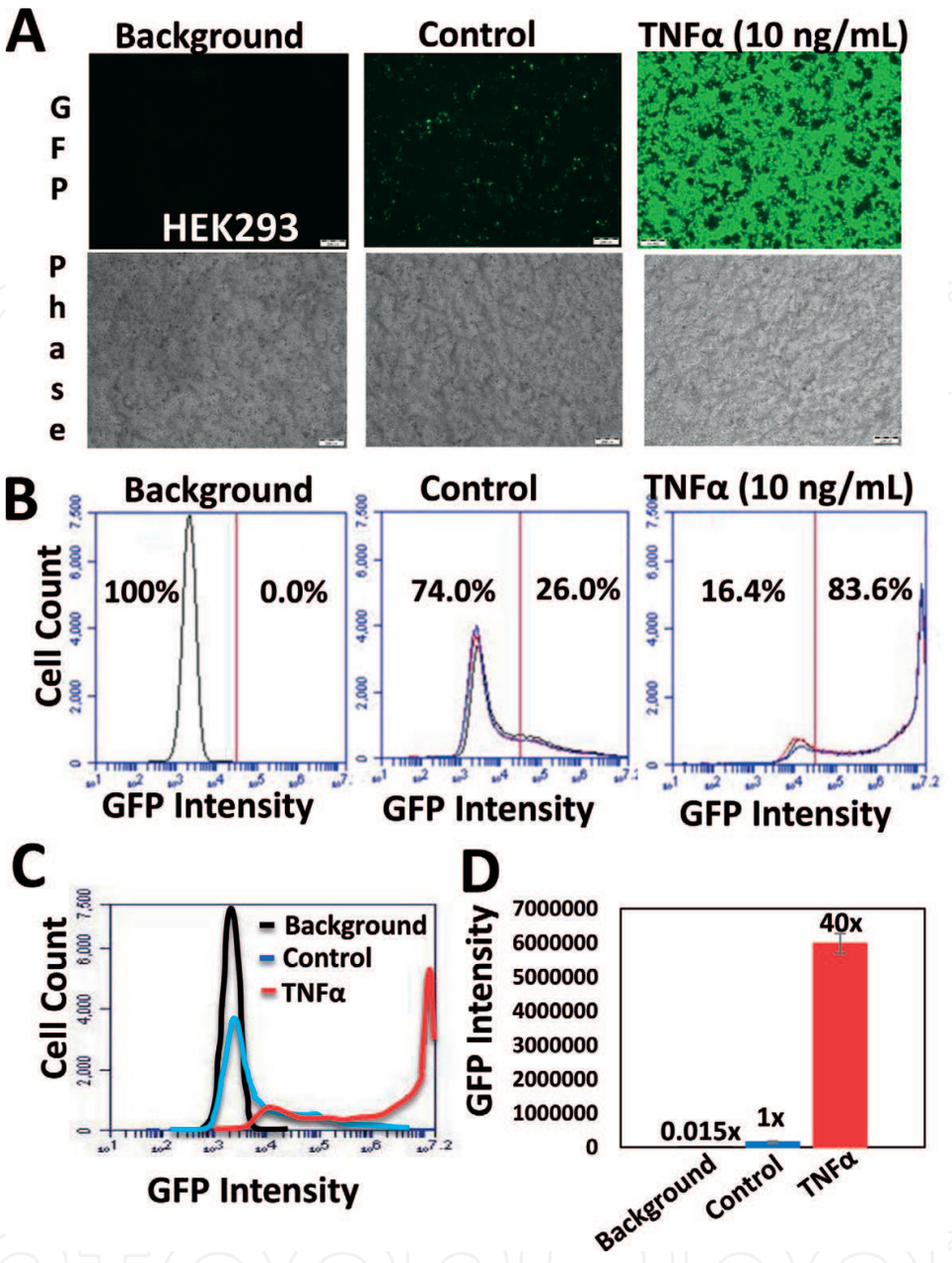

Figure 6. High-content quantification of inflammatory response by the flow cytometry. Following transduction with NFκB reporter virus (MOI = 1) or mock transduction (background control) for 24 h, HEK293 cells were switched to serum-free medium in the presence or absence (b) of TNFα (10 ng/mL) for additional 24 h. Response of individual cells was imaged by fluorescence microscopy (A) and further quantified by FACS analysis (B, C). The average response was calculated and graphed (D). The data was presented as mean ± SD, n = 3.

with a laser lamp and a GFP signal detector. As expected, TNFα treatment induced a drastic increase in the GFP intensity over control (**Figure 7A**) with a 16.7-fold increase in GFP signal measured by a microplate reader. To further examine whether our NFκB reporter can be used to monitor the inflammation response in other cell types, we transfected two additional human cell types (U87 and HepG2) with this reporter and quantified their response to TNFα treatment. Similar to HEK293 cells, we observed marked increases (9.2-fold and 18.3-fold over control) in GFP

http://dx.doi.org/10.5772/intechopen.78568

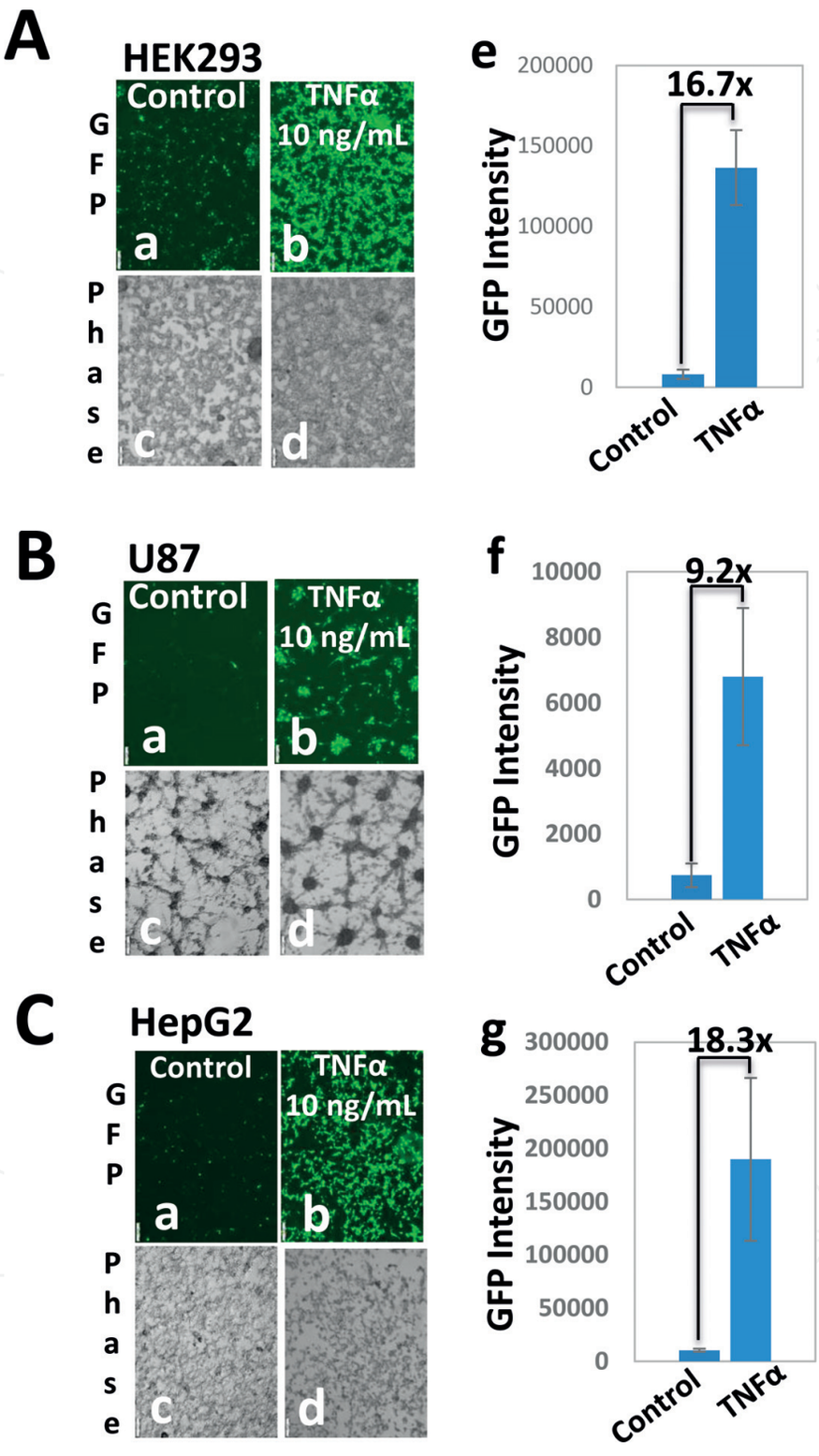

Figure 7. Quantification of inflammatory response by microplate reader. Three types of human cells were separately transfected with NF-κB reporter for 24 h and then switched to serum-free complete medium in the presence or absence of TNFα (10 ng/mL) for additional 24 h. The GFP (A–C: a, b) and phase (A–C: c, d) images were taken and the corresponding GFP intensity was further quantified by a microplate reader and graphed (e–g). The data was presented as mean ± SD, n = 3.

intensity in U87 (**Figure 7B**) and HepG2 (**Figure 7C**) cells, respectively. Together, our results validated another convenient approach for signal quantification by using less expensive Microplate reader, which is easily amenable to laboratory automation.

4. Discussion

4.1. Features of the new genetic circuit

We report the development of a new AAV-based dual-reporter circuit for live monitoring of cell signaling that is fundamental to both physiology and pathology. Our system combines two functionally complementary reporters (Gluc and GFP), which enables HTP applications and laboratory automation. The distinctive feature of this dual-reporter from our previous ones [18, 27] is the introduction of Gluc, which is a secretary form of luciferase and can be easily retrieved from conditioned medium for quantification [17]. Retaining the GFP reporter preserves the capability of both real-time imaging and single cell analysis [34]. Through comprehensive examination and validation using a fluorescence microscope, flow cytometer, and microplate reader, we demonstrated that our new system is robust and provides attractive advantages over existing methods. These advantages include a wide detection range, low background, high sensitivity and better specificity, and multiple gene delivery options.

4.2. Genetic circuit better reports cellular response with relevant physiological and pathophysiological significance

The successful development of a genetic circuit requires a sound strategy and an ability to monitor molecular singling in a highly sensitive and specific manner. To study inflammation, we chose the NFκB because it is an important transcription factor in regulating cellular responses with a rapid-activation property [43–45]. In most types of cells, NFκB exists as a dimer in the cytoplasm in an inactive status via interaction with IκB inhibitor proteins. NFκB can be activated by various inflammatory molecules, including TNFα, IL-1β, or bacterial lipopolysaccharides (LPS) [44–46]. Upon binding of these stimuli to their respective receptors, the IκB kinase becomes activated and phosphorylates IκB proteins, which in turn are ubiquitinated and degraded by proteasomes. Once the IκB is degraded, the NFκB complex is free to migrate into nucleus where it binds to its response element and turns on the expression of specific genes that mediate inflammatory responses [47, 48]. Traditionally, methods for the study of inflammation are invasive in nature. Two commonly used methods are Western blot analysis for evaluating IκB activation and RT-PCR for quantifying effector gene expression, both requiring lysis of cells. Additionally, these methods are cumbersome and low in throughput [43, 48]. To overcome these limitations, Lee et al. created a RFP- NFκB reporter cell line, which allows researchers to monitor the NFκB translocation from the cytoplasm to the nucleus [49]. Although this reporter may permit real-time monitoring, its readout is one of the early events of inflammatory signaling, namely the NFκB translocation, rather than the biological endpoint [49]. Due to the oscillation of NFkB, this process may not correlate well with the biological response. Differing from RFP-NFκB reporter, our new system monitors the transcriptional activation, the final step in

producing the biological response. Thus, our new system will produce biologically relevant data. Moreover, our dual-reporter format may preserve the signaling history at both individual cell (GFP) and population (Gluc) levels, yielding complimentary data sets as demonstrated in this study (**Figures 3**–**5**). Most importantly, the endpoint quantification is a direct measurement of NFκB activation in terms of GFP intensity or Gluc activity. Those measurements can be obtained via high content FACS analysis or laboratory automotive microplate reader, in a sensitive and specific manner.

4.3. The dual-reporter circuit is applicable to other signaling pathways

Transcriptional activation and control of gene expression is the common focal point that converges on a variety of signaling pathways. Here, we demonstrate that our dual-reporter system can be used to monitor two critical signaling pathways mediated by either by NFκB (inflammation) or AP-1 (cell proliferation and/or differentiation). By the same token, our genetic circuit can be easily modified to report other critical signaling processes such as cancer (P53 or Myc), dyslipidemia (SREBP1 or PPAR), brain development (OCT4 or PAX6) and endocrine function (ER or AR). Hence, this new genetic circuit will have wide applicability and represents a promising platform for studying cell signaling in live cell or animal models.

5. Conclusions

We developed and validated a new dual-reporter circuit for real-time monitoring and quantification of inflammatory signaling in various mammalian cells. The new system is readily amenable to noninvasive manipulations allowing high throughput applications and laboratory automation.

Acknowledgements

We thank Dr. Yan Jiang for critically reviewing the manuscript and helpful comments.

Author details

Natalie Duong†, Kevin Curley†, Mai Anh Do, Daniel Levy and Biao Lu*

*Address all correspondence to: blu2@scu.edu

Department of Bioengineering, School of Engineering, Santa Clara University, Santa Clara, California, USA

†These authors contributed equally to this work.

References

[1] Tsien RY, Miyawaki A. Seeing the machinery of live cells. Science. 1998;**280**(5371):1954-1955

[2] Zhang J, Campbell RE, Ting AY, Tsien RY. Creating new fluorescent probes for cell biology. Nature Reviews. Molecular Cell Biology. 2002;**3**(12):906-918

[3] Chalfie M, Tu Y, Euskirchen G, Ward WW, Prasher DC. Green fluorescent protein as a marker for gene expression. Science. 1994;**263**(5148):802-805

[4] Kim JB, Urban K, Cochran E, Lee S, Ang A, Rice B, Bata A, Campbell K, Coffee R, Gorodinsky A, et al. Non-invasive detection of a small number of bioluminescent cancer cells in vivo. PLoS One. 2010;**5**(2):e9364

[5] Kanno A, Yamanaka Y, Hirano H, Umezawa Y, Ozawa T. Cyclic luciferase for real-time sensing of caspase-3 activities in living mammals. Angewandte Chemie (International Ed. in English). 2007;**46**(40):7595-7599

[6] Li Z, Lee A, Huang M, Chun H, Chung J, Chu P, Hoyt G, Yang P, Rosenberg J, Robbins RC, et al. Imaging survival and function of transplanted cardiac resident stem cells. Journal of the American College of Cardiology. 2009;**53**(14):1229-1240

[7] Huang M, Chen Z, Hu S, Jia F, Li Z, Hoyt G, Robbins RC, Kay MA, Wu JC. Novel minicircle vector for gene therapy in murine myocardial infarction. Circulation. 2009;**120** (11 Suppl):S230-S237

[8] Chereau R, Tonnesen J, Nagerl UV. STED microscopy for nanoscale imaging in living brain slices. Methods. 2015;**88**:57-66

[9] Fernandez-Suarez M, Ting AY. Fluorescent probes for super-resolution imaging in living cells. Nature Reviews. Molecular Cell Biology. 2008;**9**(12):929-943

[10] Jones CT, Catanese MT, Law LM, Khetani SR, Syder AJ, Ploss A, Oh TS, Schoggins JW, MacDonald MR, Bhatia SN, et al. Real-time imaging of hepatitis C virus infection using a fluorescent cell-based reporter system. Nature Biotechnology. 2010;**28**(2):167-171

[11] Bartok E, Bauernfeind F, Khaminets MG, Jakobs C, Monks B, Fitzgerald KA, Latz E, Hornung V. iGLuc: A luciferase-based inflammasome and protease activity reporter. Nature Methods. 2013;**10**(2):147-154

[12] Shaner NC, Campbell RE, Steinbach PA, Giepmans BN, Palmer AE, Tsien RY. Improved monomeric red, orange and yellow fluorescent proteins derived from Discosoma sp. red fluorescent protein. Nature Biotechnology. 2004;**22**(12):1567-1572

[13] Tsien RY. The green fluorescent protein. Annual Review of Biochemistry. 1998;**67**:509-544

[14] Nagai T, Ibata K, Park ES, Kubota M, Mikoshiba K, Miyawaki A. A variant of yellow fluorescent protein with fast and efficient maturation for cell-biological applications. Nature Biotechnology. 2002;**20**(1):87-90

[15] Mezzanotte L, Blankevoort V, Lowik CW, Kaijzel EL. A novel luciferase fusion protein for highly sensitive optical imaging: From single-cell analysis to in vivo whole-body bioluminescence imaging. Analytical and Bioanalytical Chemistry. 2014;**406**(23):5727-5734

[16] Lorenz WW, McCann RO, Longiaru M, Cormier MJ. Isolation and expression of a cDNA encoding Renilla reniformis luciferase. Proceedings of the National Academy of Sciences of the United States of America. 1991;**88**(10):4438-4442

[17] Wurdinger T, Badr C, Pike L, de Kleine R, Weissleder R, Breakefield XO, Tannous BA. A secreted luciferase for ex vivo monitoring of in vivo processes. Nature Methods. 2008;**5**(2): 171-173

[18] Afshari A, Uhde-Stone C, Lu B. Live visualization and quantification of pathway signaling with dual fluorescent and bioluminescent reporters. Biochemical and Biophysical Research Communications. 2014;**448**(3):281-286

[19] Tay S, Hughey JJ, Lee TK, Lipniacki T, Quake SR, Covert MW. Single-cell NF-kappaB dynamics reveal digital activation and analogue information processing. Nature. 2010;**466**(7303): 267-271

[20] Stickney Z, Losacco J, McDevitt S, Zhang Z, Lu B. Development of exosome surface display technology in living human cells. Biochemical and Biophysical Research Communications. 2016;**472**(1):53-59

[21] Badr CE, Hewett JW, Breakefield XO, Tannous BA. A highly sensitive assay for monitoring the secretory pathway and ER stress. PLoS One. 2007;**2**(6):e571

[22] Koutsoudakis G, Perez-del-Pulgar S, Gonzalez P, Crespo G, Navasa M, Forns X. A Gaussia luciferase cell-based system to assess the infection of cell culture- and serum-derived hepatitis C virus. PLoS One. 2012;**7**(12):e53254

[23] Canaria CA, Lansford R. Advanced optical imaging in living embryos. Cellular and Molecular Life Sciences. 2010;**67**(20):3489-3497

[24] Uhde-Stone C, Huang J, Lu B. A robust dual reporter system to visualize and quantify gene expression mediated by transcription activator-like effectors. Biological Procedures Online. 2012;**14**(1):8

[25] Afshari A, Uhde-Stone C, Lu B. A cooled CCD camera-based protocol provides an effective solution for in vitro monitoring of luciferase. Biochemical and Biophysical Research Communications. 2015;**458**(3):543-548

[26] Tannous BA. Gaussia luciferase reporter assay for monitoring biological processes in culture and in vivo. Nature Protocols. 2009;**4**(4):582-591

[27] Zhang Z, Stickney Z, Duong N, Curley K, Lu B. AAV-based dual-reporter circuit for monitoring cell signaling in living human cells. Journal of Biological Engineering. 2017;**11**:18

[28] Tannous BA, Kim DE, Fernandez JL, Weissleder R, Breakefield XO. Codon-optimized Gaussia luciferase cDNA for mammalian gene expression in culture and in vivo. Molecular Therapy. 2005;**11**(3):435-443

[29] Uhde-Stone C, Sarkar N, Antes T, Otoc N, Kim Y, Jiang YJ, Lu B. A TALEN-based strategy for efficient bi-allelic miRNA ablation in human cells. RNA. 2014;**20**(6):948-955

[30] Grimm D, Lee JS, Wang L, Desai T, Akache B, Storm TA, Kay MA. In vitro and in vivo gene therapy vector evolution via multispecies interbreeding and retargeting of adeno-associated viruses. Journal of Virology. 2008;**82**(12):5887-5911

[31] Potter M, Lins B, Mietzsch M, Heilbronn R, Van Vliet K, Chipman P, Agbandje-McKenna M, Cleaver BD, Clement N, Byrne BJ, et al. A simplified purification protocol for recombinant adeno-associated virus vectors. Molecular therapy. Methods & Clinical Development. 2014;**1**:14034

[32] Zolotukhin S, Potter M, Zolotukhin I, Sakai Y, Loiler S, Fraites TJ, Chiodo VA, Phillipsberg T, Muzyczka N, Hauswirth WW, et al. Production and purification of serotype 1, 2, and 5 recombinant adeno-associated viral vectors. Methods. 2002;**28**(2):158-167

[33] Sengupta R, Mukherjee C, Sarkar N, Sun Z, Lesnik J, Huang J, Lu B. An optimized protocol for packaging Pseudotyped integrase defective lentivirus. Biological Procedures Online; **2017, 18**:14

[34] Wiedenmann J, Oswald F, Nienhaus GU. Fluorescent proteins for live cell imaging: Opportunities, limitations, and challenges. IUBMB Life. 2009;**61**(11):1029-1042

[35] Kellogg RA, Tay S. Noise facilitates transcriptional control under dynamic inputs. Cell. 2015;**160**(3):381-392

[36] Lu B, Lu Y, Moser AH, Shigenaga JK, Grunfeld C, Feingold KR. LPS and proinflammatory cytokines decrease lipin-1 in mouse adipose tissue and 3T3-L1 adipocytes. American Journal of Physiology. Endocrinology and Metabolism. 2008;**295**(6):E1502-E1509

[37] Lu B, Moser A, Shigenaga JK, Grunfeld C, Feingold KR. The acute phase response stimulates the expression of angiopoietin like protein 4. Biochemical and Biophysical Research Communications. 2010;**391**(4):1737-1741

[38] Lu B, Moser AH, Shigenaga JK, Feingold KR, Grunfeld C. Type II nuclear hormone receptors, coactivator, and target gene repression in adipose tissue in the acute-phase response. Journal of Lipid Research. 2006;**47**(10):2179-2190

[39] Johnston SR, Lu B, Scott GK, Kushner PJ, Smith IE, Dowsett M, Benz CC. Increased activator protein-1 DNA binding and c-Jun NH2-terminal kinase activity in human breast tumors with acquired tamoxifen resistance. Clinical Cancer Research. 1999;**5**(2):251-256

[40] Burger C, Gorbatyuk OS, Velardo MJ, Peden CS, Williams P, Zolotukhin S, Reier PJ, Mandel RJ, Muzyczka N. Recombinant AAV viral vectors pseudotyped with viral capsids from serotypes 1, 2, and 5 display differential efficiency and cell tropism after delivery to different regions of the central nervous system. Molecular Therapy. 2004;**10**(2):302-317

[41] Xiao X, Li J, Samulski RJ. Efficient long-term gene transfer into muscle tissue of immunocompetent mice by adeno-associated virus vector. Journal of Virology. 1996;**70**(11):8098-8108

[42] Zeltner N, Kohlbrenner E, Clement N, Weber T, Linden RM. Near-perfect infectivity of wild-type AAV as benchmark for infectivity of recombinant AAV vectors. Gene Therapy. 2010;**17**(7):872-879

[43] Hoffmann A, Baltimore D. Circuitry of nuclear factor kappaB signaling. Immunological Reviews. 2006;**210**:171-186

[44] Cheong R, Bergmann A, Werner SL, Regal J, Hoffmann A, Levchenko A. Transient IkappaB kinase activity mediates temporal NF-kappaB dynamics in response to a wide range of tumor necrosis factor-alpha doses. The Journal of Biological Chemistry. 2006;**281**(5):2945-2950

[45] Covert MW, Leung TH, Gaston JE, Baltimore D. Achieving stability of lipopolysaccharide-induced NF-kappaB activation. Science. 2005;**309**(5742):1854-1857

[46] Muzio M, Ni J, Feng P, Dixit VM. IRAK (Pelle) family member IRAK-2 and MyD88 as proximal mediators of IL-1 signaling. Science. 1997;**278**(5343):1612-1615

[47] Nelson DE, Ihekwaba AE, Elliott M, Johnson JR, Gibney CA, Foreman BE, Nelson G, See V, Horton CA, Spiller DG, et al. Oscillations in NF-kappaB signaling control the dynamics of gene expression. Science. 2004;**306**(5696):704-708

[48] Hoffmann A, Levchenko A, Scott ML, Baltimore D. The IkappaB-NF-kappaB signaling module: Temporal control and selective gene activation. Science. 2002;**298**(5596):1241-1245

[49] Lee TK, Denny EM, Sanghvi JC, Gaston JE, Maynard ND, Hughey JJ, Covert MW. A noisy paracrine signal determines the cellular NF-kappaB response to lipopolysaccharide. *Science Signaling*. 2009;**2**(93):ra65

IntechOpen